CHEMISTRY AND CHEMICAL ENGINEERING

Volume 2023 | Number 2 Article 5

March 2024

STUDY OF NANO PHASE-SEPARATION IN Cu51Zr14 ALLOY

Anna STRIJEVSKAYA
Uzbek-Japanese Youth Innovation Center, Tashkent, Uzbekistan, astrijevskaya@mail.ru

Zukhra KADIROVA
Uzbek-Japanese Youth Innovation Center, Tashkent, Uzbekistan, zuhra_kadirova@yahoo.com

Shakhlo DAMINOVA
Uzbek-Japanese Youth Innovation Center, Tashkent, Uzbekistan; National University of Uzbekistan, Tashkent, Uzbekistan, daminova_sh@mail.ru

Masahiro MIYAUCHI
Tokyo Institute of Technology, Tokyo, Japan, mmiyauchi@ceram.titech.ac.jp

Ayako HASHIMOTO
National Institute for Materials Science, Tsukuba, Ibaraki, Japan; Graduate School of Pure and Applied Sciences, University of Tsukuba, Tsukuba, Ibaraki, Japan, HASHIMOTO.Ayako@nims.go.jp

See next page for additional authors

Recommended Citation

STRIJEVSKAYA, Anna; KADIROVA, Zukhra; DAMINOVA, Shakhlo; MIYAUCHI, Masahiro; HASHIMOTO, Ayako; WEN, Yu; and ABE, Hideki (2024) "STUDY OF NANO PHASE-SEPARATION IN Cu51Zr14 ALLOY," *CHEMISTRY AND CHEMICAL ENGINEERING*: Vol. 2023: No. 2, Article 5.
DOI: 10.34920/cce202325
Available at: https://cce.researchcommons.org/journal/vol2023/iss2/5

STUDY OF NANO PHASE-SEPARATION IN Cu51Zr14 ALLOY

Authors

Anna STRIJEVSKAYA, Zukhra KADIROVA, Shakhlo DAMINOVA, Masahiro MIYAUCHI, Ayako HASHIMOTO, Yu WEN, and Hideki ABE

STUDY OF NANO PHASE-SEPARATION IN $Cu_{51}Zr_{14}$ ALLOY

Anna STRIJEVSKAYA[1] (astrijevskaya@mail.ru), Zukhra KADIROVA[1] (zuhra_kadirova@yahoo.com), Shakhlo DAMINOVA[1,2] (daminova_sh@mail.ru), Masahiro MIYAUCHI[3] (mmiyauchi@ceram.titech.ac.jp), Ayako HASHIMOTO[4,5] (HASHIMOTO.Ayako@nims.go.jp), Yu WEN[4,5] (wenyu93@outlook.com), Hideki ABE[4,6] (abe.hideki@nims.go.jp)
[1]Uzbek-Japanese Youth Innovation Center, Tashkent, Uzbekistan
[2]National University of Uzbekistan, Tashkent, Uzbekistan
[3]Tokyo Institute of Technology, Tokyo, Japan
[4]National Institute for Materials Science, Tsukuba, Ibaraki, Japan.
[5]Graduate School of Pure and Applied Sciences, University of Tsukuba, Tsukuba, Ibaraki, Japan
[6]Graduate School of Science and Technology, Saitama University, Saitama, Japan

The aim of this work is to obtain new materials for electrocatalysis based on nanostructured copper and zirconium alloys. New nano phase-separated material Cu#ZrO_2 deducted from conventional $Cu_{51}Zr_{14}$ alloy precursor was developed. The materials' characteristics were determined using FE-SEM, STEM, XRD and electrochemical methods. The optimal conditions for the nano separation in alloy system have been established. Under conditions of heat treatment evolution of phase separation occurs through the exchange events between atoms and inward-outward migration of cations and anions. The electrochemical and BET surface area was determined. Based on the processing of the electrochemical data Cu#ZrO_2 demonstrates promising potential for electrocatalytic activity.

Keywords: alloys, phase separation, ZrO_2, Cu, electrochemistry

ИЗУЧЕНИЕ НАНО-ФАЗНОЙ СЕПАРАЦИИ В СПЛАВЕ $Cu_{51}Zr_{14}$

Анна СТРИЖЕВСКАЯ[1] (astrijevskaya@mail.ru), Зухра КАДИРОВА[1] (zuhra_kadirova@yahoo.com), Шахло ДАМИНОВА[1,2] (daminova_sh@mail.ru), Масахиро МИЯУЧИ[3] (mmiyauchi@ceram.titech.ac.jp), Аяко ХАШИМОТО[4,5] (HASHIMOTO.Ayako@nims.go.jp), Ю ВЕН[4,5] (wenyu93@outlook.com), Хидеки АБЭ[4,6] (abe.hideki@nims.go.jp)
[1]Узбекско-японский молодежный центр инноваций, Ташкент, Узбекистан
[2]Национальный университет Узбекистана, Ташкент, Узбекистан
[3]Токийский технологический институт, Токио, Япония
[4]Национальный институт материаловедения, Цукуба, Ибараки, Япония
[5]Высшая школа чистых и прикладных наук, Университет Цукуба, Цукуба, Ибараки, Япония
[6]Высшая школа науки и технологий, Университет Сайтама, Сайтама, Япония

Цель работы получение новых материалов для электрокатализа на основе наноструктурированных сплавов меди и циркония. Разработан новый нанофазовый материал Cu#ZrO_2, полученный из исходного сплава $Cu_{51}Zr_{14}$. Характеристики материала были определены методами FE-SEM, STEM, XRD и циклической вольтометрией. Установлены оптимальные условия для наноразделения в системе сплавов. В условиях термической обработки развитие фазового разделения происходит за счет обменных актов между атомами и миграции катионов и анионов внутрь-наружу. Определяли электрохимическую площадь и площадь поверхности по БЭТ. На основании обработки электрохимических данных Cu#ZrO_2 демонстрирует многообещающий потенциал электрокаталитической активности.

Ключевые слова: сплавы, фазовое разделение, ZrO_2, Cu, электрохимия

$Cu_{51}Zr_{14}$ QOTISHMASIDA NANO-FAZALARNI AJRATISHNI O'RGANISH

Anna STRIJEVSKAYA[1] (astrijevskaya@mail.ru), Zukhra KADIROVA[1] (zuhra_kadirova@yahoo.com), Shaxlo DAMINOVA[1,2] (daminovash@mail.ru), Masahiro MIYAUCHI[3] (mmiyauchi@ceram.titech.ac.jp), Ayako HASHIMOTO[4,5] (HASHIMOTO.Ayako@nims.go.jp), Yu VEN[4,5] (wenyu93@outlook.com), Xideki ABE[4,6] (abe.hideki@nims.go.jp)
[1]O'zbekiston-Yaponiya yoshlar innovatsiya markazi, Toshkent, O'zbekiston
[2]O'zbekiston Milliy universiteti, Toshkent, O'zbekiston
[3]Tokio texnologiya instituti, Tokio, Yaponiya
[4]Milliy Materialshunoslik instituti, Tsukuba, Ibaraki, Yaponiya
[5]Sof va amaliy fanlar oliy maktabi, Tsukuba universiteti, Tsukuba, Ibaraki, Yaponiya
[6]Saitama universiteti, Fan va texnologiya oliy maktabi, Saitama, Yaponiya

Ushbu ishning maqsadi nanostrukturali mis va sirkoniy qotishmalari asosida elektrokataliz uchun yangi materiallarni olishdir. An'anaviy Cu_{51}Zr14 qotishma prekursoridan ajratilgan yangi nanofazali Cu#ZrO_2 materiali ishlab chiqildi. Materiallarning xususiyatlari FE-SEM, STEM, XRD va elektrokimyoviy usullar yordamida aniqlandi. Qotishma tizimida nanofazali ajratish uchun optimal sharoitlar yaratildi. Termik ishlov berish sharoitida fazalarni ajratish atomlar, kationlar va anionlarning ichkaridan tashqariga ko'chishi o'rtasidagi almashinish hodisalari orqali sodir bo'ladi. Elektrokimyoviy va BET sirt maydoni aniqlandi. Elektrokimyoviy ma'lumotlarni qayta ishlash asosida Cu#ZrO_2 elektrokatalitik faollik uchun istiqbolli salohiyatni namoyish etadi.

Kalit so'zlar: qotishmalar, fazalarni ajratish, ZrO_2, Cu, elektrokimyo

DOI: 10.34920/cce202325

Introduction

Recently, a new class of catalysts for dry methane reforming and $NO_{(x)}$ conversion [1] was developed by H. Abe's group via nano-phase separation occurring during the heat treatment of precursor alloy in oxidative-reductive gas mixture. Obtained catalysts possess substantial durability, the ability to work under low temperatures and improved catalytic activity due to sophisticated entangled nanofiber morphology with an average size of 10 nm. This kind of morphology ensures high distribution of active sites over the catalyst, while the oxide part serves as a matrix efficient to prevent sintering and aggregation. Moreover, nano phase separation allows obtaining monodispersed porosity with such durable metals as Rh [2]. However, to the best of our knowledge, up to now due to novelty of the technique, the purposeful nano phase-separation was mostly used for catalysts containing precious and rare-earth metals, such as Pt, Ce, Y and Rh. Though, recently Penner showed the mechanism of self-activation of $Cu_{51}Zr_{14}$ alloy during methanol steam reforming [3], the obtained phase separation was in the micrometer scale, which greatly affects catalytic activity. Thus, inspired by the nano phase separation technique and potential abilities of Cu-ZrO_2 systems, here we report a study on the nano phase separation in $Cu_{51}Zr_{14}$ alloy. Resulted Cu#ZrO_2 system possesses neat distribution of Cu and zirconia phases with approximate width of 10 nm. This even and abundant distribution of catalytically active sites ensures electrochemical surface area of 10.9 m^2/g, which is 50 times larger than the surface area of commercial Cu powder.

Materials and Methods

Synthesis of $Cu_{51}Zr_{14}$ alloy precursor. An ingot of $Cu_{51}Zr_{14}$ precursor alloy was obtained by arc-melting of Cu and Zr metals in argon (Ar) atmosphere. For this process, Cu foil (99.99%, Nilaco corporation) and Zr chunks (99.99%, Nilaco Corporation) were weighted in a molar ratio at 51:14 placed on a water-cooled copper hearth and subjected to a plasma arc torch. $Cu_{51}Zr_{14}$ precursor alloy ingot was powdered with an agate mortar in air and sieved to adjust the size of particles between 40 and 50 mm. The $Cu_{51}Zr_{14}$ powder was placed on a ceramic boat and heated at 400 °C for 12 hours in a stream of mixture gases of carbon monoxide (CO)- and oxygen (O_2) at a molar ratio of 2:1 and a total flow rate of 100 $mLmin^{-1}$. The blackish gray $Cu_{51}Zr_{14}$ powder was converted into a dark-purple nanocomposite of metal Cu and zirconium oxide (ZrO_2), *i.e.*, Cu#ZrO_2.

Characterization. The synthesized Cu#ZrO_2 material as well as the $Cu_{51}Zr_{14}$ precursor alloy were characterized by powder X-ray diffraction (pXRD) over a 2q range of 20 to 80 degrees with a Rigaku SmartLab diffractometer equipped with a D/teX Ultra detector. The elemental composition and crystallographic structure of the samples were identified with a scanning transmission electron microscope (STEM, JEM-ARM200F, JEOL) imaging operating at an acceleration voltage of 200 kV. A field-emission scanning electron microscope (FE -SEM, JSM-7500F (JEOL)) was used to observe the external morphology of the materials. The BET measurements were conducted on Micromeritics MicroActive TriStar II Plus and electrochemical test were conducted on Hokuto Denko HZ-7000.

Results and Discussions

X-ray diffraction measurement (Figure 1) of catalyst powder coincides with patterns of metallic Cu and mixture of monoclinic and tetragonal ZrO_2- typical crystal structure for internally oxidized Cu-Zr alloys [4, 5] beside this there were also

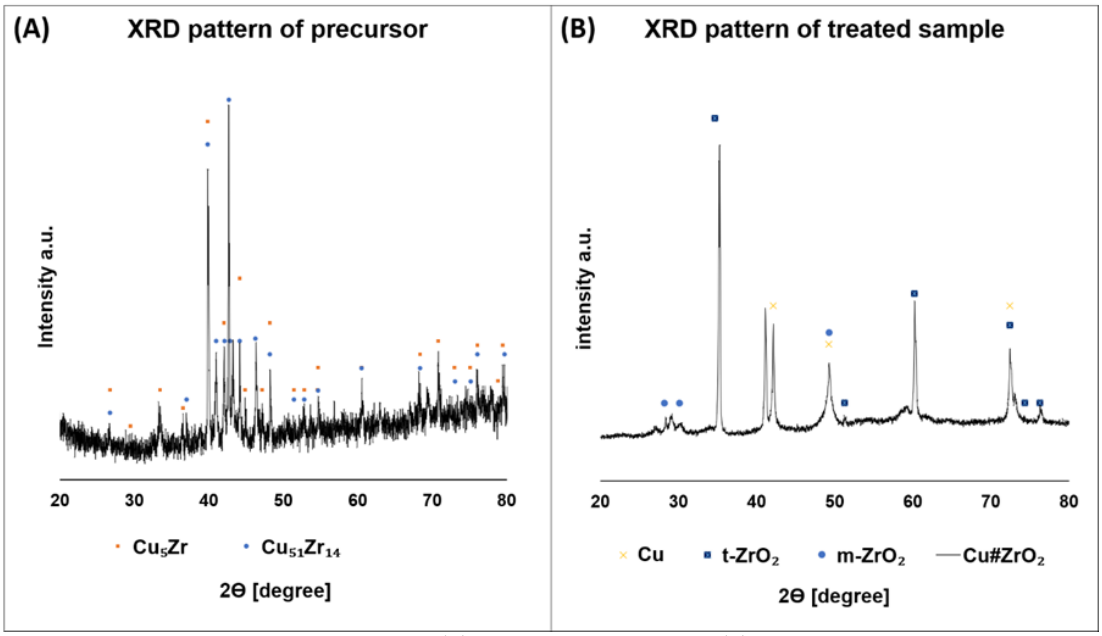

Figure 1. pXRD patterns for (A) $Cu_{51}Zr_{14}$ alloy precursor and (B) post-treated Cu#ZrO_2.

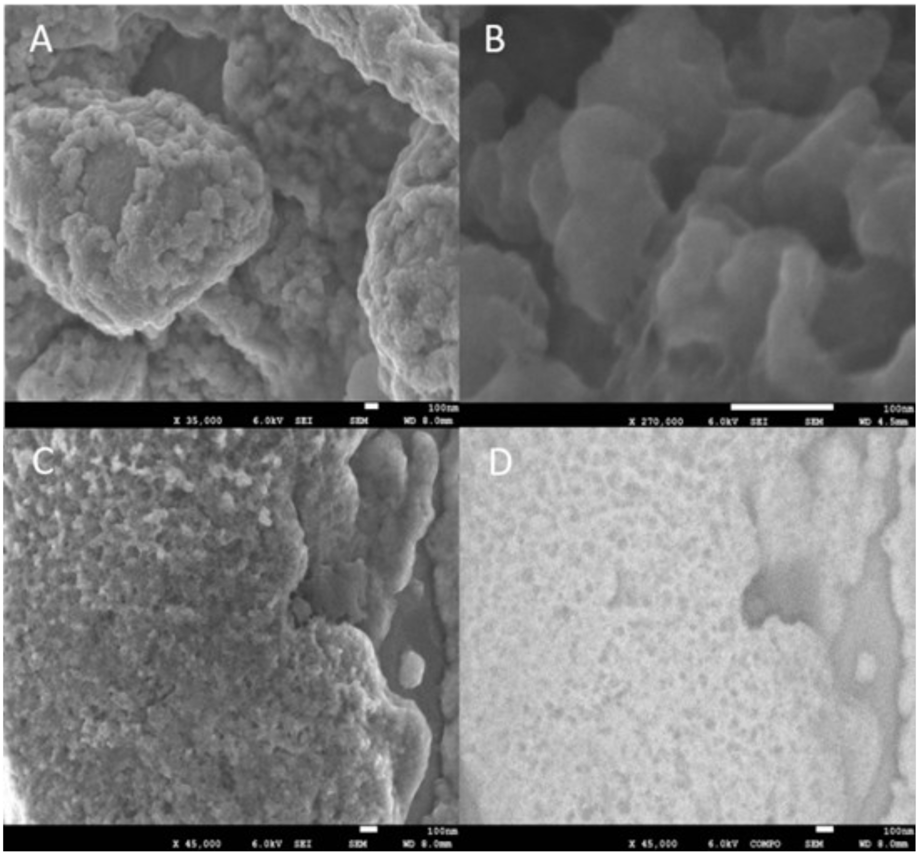

Figure 2. FE-SEM images of Cu#ZrO_2 grains A- overall secondary electron image of the particle. B- magnified image of spikes. C- image of the particles, representing prominent pattern. D-back scattered electron image, showing presence of two phases.

noticed some impurities of Cu_2O, produced, probably, during grinding in mortar and exposing powder to the air. Formation of tetragonal ZrO_2 is thermodynamically less favorable, as it needs to be stabilized externally by dopants or internally by oxygen vacancies. Same time, Cu is known to stabilize tetragonal phase zirconia dioxide in conditions of methanol steam reforming reaction. Therefore, we surmise that similarity in the lattice constant of cubic Cu and t-ZrO_2 acted energetically favorably by epitaxial stabilization [6]. Beside this, according to the phase distribution and average width of each phase, tetragonal zirconia might have been stabilized by size factor, as it was mentioned by Vahidshad [7].

FE-SEM images of the sample at 45000 magnifications (Figure 2. C-D) show maze pattern morphology with prominent spikes, that in higher magnification appear to have cubic shape. According to the back scattered image the white phase can be attributed to ZrO_2 and dark- to copper.

Diffraction pattern, obtained from ADF-STEM (Figure 3) taken near the surface layer of catalyst grain indicates d spacing of (010) plane ZrO_2 phase as d (200) 0,29 nm, d (111) 0,24 nm, which constitutes, as it was mentioned before, formation of tetragonal meta stable zirconia oxide phase. Result of calculation of lattice parameter (Table 1) perfectly matches with tetragonal crystal structure, which is also confirmed by reflections of crystallographic planes. From the equation for calculation tetragonal lattice we determined c value to be equal 0,5176 nm and a 0,3606 nm for t-ZrO_2, space group P42/nmc, a little bit compressed tetragonal unit cell with volume of 0,067nm^3.

For tetragonal: $$\frac{1}{d^2}=\frac{h^2+k^2}{\mathrm{a}^2}+\frac{l^2}{c^2}$$

For FCC: $$\frac{1}{d^2}=\frac{h^2+k^2+l^2}{\mathrm{a}^2}$$

That gives us value of 0,426 nm for Cu_2O that is a little bit larger, than reported value for Cu_2O [8] and which explains the XRD peaks shift to higher angle. As m-ZrO_2 phase constitutes only minor part of the sample we did not perform calculation for its lattice parameters [9].

The reaction rout of the heat treatment of $Cu_{51}Zr_{14}$ is as follows:

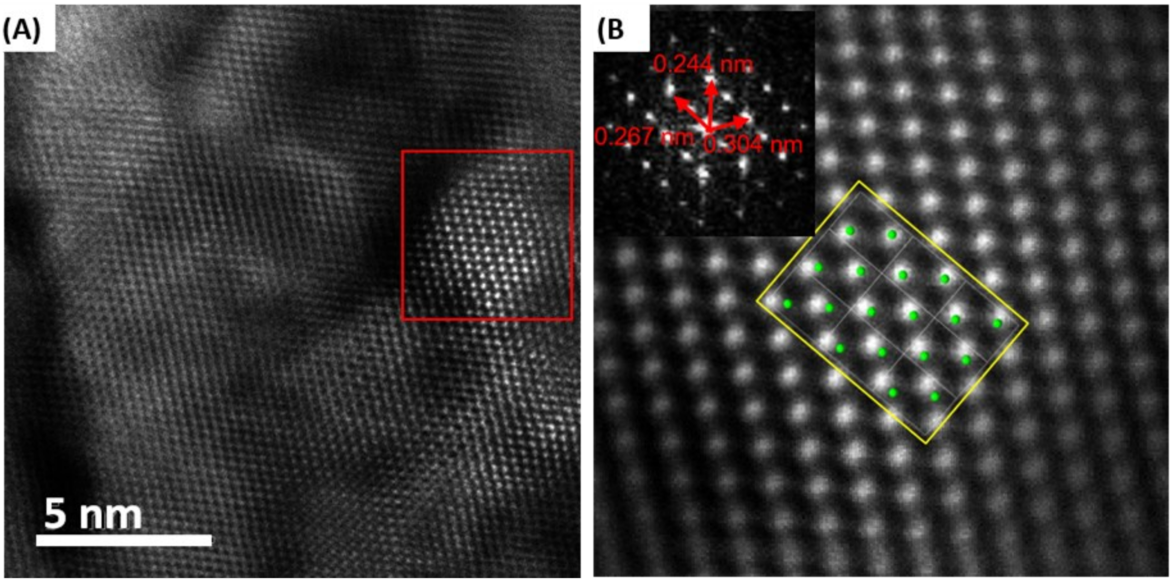

Figure 3. ADF-STEM taken from red square area image showing a lamellar structure in Cu#ZrO$_2$ A). A high resolution ADF-STEM image at the Cu-ZrO$_2$ boundary and a of FFT pattern in the inset (B).

$$4Cu_{51}Zr_{14}+107O_2=102Cu_2O+56ZrO_2$$

$$Cu_2O+CO=2Cu+CO_2$$

The oxidation mechanism of alloys containing Cu and Zr was thoroughly studied by Wang [10] and Tam [11], in accordance with this ZrO$_2$ as n-type anion deficient oxide, which growth happens by inward diffusion of oxygen anions. While Cu$_2$O is p-type cation deficient oxide whose cations migrate outwards through cation vacancies to the interface between sample and reactant gas mixture. This was earlier confirmed by Kai's study with Pt marker [12], that showed that after the oxidation Pt always

Table 1

Miller Indices and d-spacing for Cu#ZrO$_2$

2θ [°]	Miller Indices			Intensity	d-spacing [nm]
	h	k	l		
Cu cubic					
43.282	1	1	1	100	0.2088
50.41	2	0	0	45	0.1809
74.068	2	2	0	21	0.1279
89.864	3	1	1	20	0.1091
95.068	2	2	2	7	0.1044
Cu$_2$O cubic					
29.562	1	1	0	100	0.3018
36.418	1	1	1	13	0.2464
42.304	2	0	0	6	0.2134
52.458	2	1	1	28	0.1743
61.374	2	2	0	17	0.1509
69.584	3	1	0	9	0.135
73.518	3	1	1	4	0.1287
ZrO$_2$ tetragonal					
34.624	0	0	2	48	0.2588
35.151	1	1	0	1	0.255
50.172	1	1	2	1	0.1817
50.564	2	0	0	100	0.1803
62.739	2	0	2	33	0.148
73.059	0	0	4	11	0.1294
74.315	2	2	0	23	0.1275
84.655	2	2	2	13	0.1144

located outside. However, our catalyst was found to be evenly nano phase separated without formation of core-shell structure, that could have been expected due to the aforementioned mechanism. Wang also suggested that formation of ZrO_2 happens not only due to inward migration of oxygen anions but also by outward diffusion of Zr. Moreover, as transformation of t-ZrO_2 to monoclinic phase was noticed to be suppressed at temperatures around 673 K [10, 13] we can suppose that formation of m-ZrO_2 occurred by secondary oxidation of Zr by reacting with cuprous oxide.

Generally, geometrical area of electrode does not coincide with its true area due to high porosity or/and small particles of catalysts. Furthermore, total area, that can be correlated to the porosity of sample and measured by nitrogen adsorption can be not the same as its catalytically active area. Thus, electrochemical surface area should be measured to determine the true active area of the catalyst. Among different methods of electrochemical surface area determination, double layer capacitance method via cyclic voltammetry is simple yet reproducible way of quantification. For this the sequence of CV scans in non-faradaic region are plotted as function of scan rate. Then, double layer capacitance C_{dl} is estimated from the slope of the linear regression between current densities in the middle of potential window versus scan rate. C_s stands for specific capacitance of standard electrode on a unit surface area, which, based on the existing literature, can be taken as 0,02 F/cm^2 [14-16].

For the purpose of correct estimation of active catalyst surface, we conduct electrochemical active surface area (ECSA) measurement by the double layer capacitance method. For this 0,1M $KHCO_3$ solution with pH 6,8, bubbled by nitrogen, served as electrolyte, carbon paper with average loading of 5 mg of catalyst was exploited as a working electrode and Pt-wire as a counter electrode. The potential window of non-faradaic region was chosen in the range of 0.0 – -0.1V. The value of 0,02 mF/cm^2 was used as the reference specific capacitance.

From our calculations, the ECSA for Cu#ZrO_2 was estimated as 10,9 m^2/g, (Fig. 4) while BET data results only in 1,64 m^2/g. The high ECSA can be attributed to small size of Cu particles and high distribution of them on the surface of catalyst's grain. The same procedure was applied for Cu powder, used as a reference in and the value of ECSA was equal to 214,7 cm^2/g.

Conclusions

In conclusion, nanophase-separated Cu#ZrO_2 was successfully obtained by internal oxidation of $Cu_{51}Zr_{14}$ precursor alloy. Microscopic characterizations have demonstrated that the Cu#ZrO_2 material consists of nanometer-thick intertwined Cu metal and tetragonal ZrO_2, leading to a stable and widespread Cu-ZrO_2 interface. The

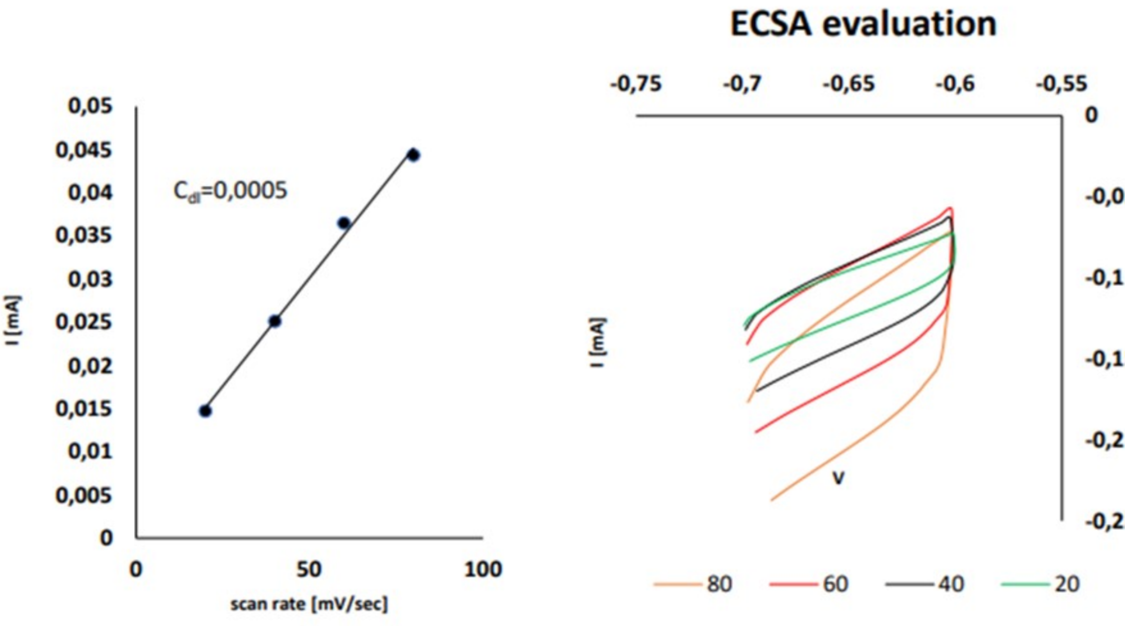

Figure 4. Electrochemical active surface area determination for Cu#ZrO_2 taken in 0.1 M $KHCO_3$.

results of electrochemical surface area determination show the high active surface area related to even distribution of nano-sized Cu in zirconia matrix. Overall, the new material is potentially capable of serving as electrocatalyst and can be applied for various catalytic reactions.

Acknowledgements

AS thankful for scholarship and financial support to Japan International Cooperation Agency (JICA) and MIRAI Fund.

REFERENCES

1. Tanabe T., Imai T., Tokunaga T., Arai S., Yamamoto Y., Ueda S., ... & Abe H. Nanophase-separated Ni 3 Nb as an automobile exhaust catalyst. *Chemical science*. 2017, 8(5), 3374-3378. DOI: 10.1039/C6SC05473K
2. Najib A.S.B.M., Peng X., Hashimoto A., Shoji S., Iida T., Bai Y., Abe H. Mesoporous Rh Emerging from Nanophase-separated Rh-Y Alloy. *Chemistry–An Asian Journal*. 2019, 14(16), 2802-2805. DOI: 10.1002/asia.201900542
3. Penner S., Kheyrollahi Nezhad P.D. Steering the Catalytic Properties of Intermetallic Compounds and Alloys in Reforming Reactions by Controlled in Situ Decomposition and Self-Activation. *ACS catalysis*, 2021, 11(9),5271-5286. DOI: 10.1021/acscatal.1c00718
4. Hietala J., Vuori A., Johnsson P., Pollari I., Reutemann W., Kieczka H. Ullmann's Encyclopedia of Industrial Chemistry. s.l. : *American Cancer Society*, 2016, 1-22. DOI:10.1002/14356007.o17_o02
5. Platt A., Frankel P., Gass M., Howells R., Preuss M. Finite element analysis of the tetragonal to monoclinic phase transformation during oxidation of zirconium alloys. *Journal of Nuclear Materials*, 2014, 454(1-3), 290-297. DOI: 10.1016/j.jnucmat.2014.08.020
6. Penner S. How the in situ monitoring of bulk crystalline phases during catalyst activation results in a better understanding of heterogeneous catalysis. *CrystEngComm*. 2021, 23(37), 6470-6480. DOI: 10.1039/D1CE00817J
7. Vahidshad Y., Abdizadeh H., Baharvandi H.R., Baseri, M.A. Structural and morphology of nanopowders copper-stabilized zirconia. *Surface Review and Letters*. 2009, 16(4), 569-577. DOI:10.1142/S0218625X09012962
8. Korzhavyi P.A., Johansson B. *Literature review on the properties of cuprous oxide Cu {sub 2} O and the process of copper oxidation.* Technical Report TR-11-08. Stockholm, 2011.
9. Hermann K,. *Crystallography and Surface Structure: An Introduction for Surface Scientists and Nanoscientists*. s.l. : WILEY-VCH Verlag GmbH & Co. KGaA, Weinheim, 2011. pp. 265-266. ISBN: 978-3-527-41012-5
10. Zhengpei Miao, Pei Hu, Chuanye Nie, Huan Xie, Wenli Fu, Qing Li. ZrO_2 nanoparticles anchored on nitrogen-doped carbon nanosheets as efficient catalyst for electrochemical CO_2 reduction. *Journal of Energy Chemistry*. 2019, 38, 114-118. DOI:10.1016/j.jechem.2019.01.010
11. Ju L., Tan X., Mao X., Gu Y., Smith S., Du A., Kou L. Controllable CO_2 electrocatalytic reduction via ferroelectric switching on single atom anchored In_2Se_3 monolayer. *Nature communications*. 12, 2021, 5128.
12. Nieh, T. G., Schuh, C., Wadsworth, J., & Li, Y. Strain rate-dependent deformation in bulk metallic glasses. *Intermetallics.,* 2002, 10(11-12), 1177-1182.
13. Wang B., Huang D. Y., Chen Z., Prud'homme N., Ji V. Oxidation kinetic and diffusion mechanism study of a Zr-based bulk metallic glass alloy. Trans Tech Publications Ltd. *In Materials Science Forum*. 2011. 675, 193-196. DOI: 10.4028/www.scientific.net/MSF.675-677.193
14. Tam C.Y., Shek C.H. Oxidation behavior of $Cu_{60}Zr_{30}Ti_{10}$ bulk metallic glass. *Journal of materials research.* 2005, 20(6), 1396-1403.
15. Ghosh, S., Mathews, T., Gupta, B., Das, A., Krishna, N. G., & Kamruddin, M. Supercapacitive vertical graphene nanosheets in aqueous electrolytes. *Nano-structures & Nano-objects*, 2017, 10, 42-50.
16. Bikkarolla, S. K., Cumpson, P., Joseph, P., & Papakonstantinou, P. Oxygen reduction reaction by electrochemically reduced graphene oxide. *Faraday discussions,* 2014, 173, 415-428.